

High precision pulsar astrometry and its applications

Walter Brisen

National Radio Astronomy Observatory, PO Box O, Socorro, NM 87801, USA

Abstract. Very long baseline interferometry (VLBI) is a radio astronomy technique that allows imaging and astrometry at milliarcsecond or better resolution. The last decade has seen improvements in VLBI techniques and equipment which have enabled precision astrometry of pulsars. Most notably, VLBI arrays have become more sensitive and calibration has become more accurate. Pulsar astrometry using VLBI can readily yield a proper motion and in many cases a trigonometric parallax as well. These observables have numerous applications which justify the difficulty of the measurements. The goals of pulsar astrometry include: 1. determination of the distribution of pulsar birth velocities, a critical probe of supernova asymmetry; 2. improvement in understanding of the ISM through observations of pulsar bow shocks, interstellar scattering, and timing dispersion measures; and 3. understanding characteristics of individual pulsars though knowledge of their distance and velocity. I will discuss these science cases, some recent results, and prospects for better astrometry in the near future.

1. Introduction

Neutron stars are extreme astrophysical objects exhibiting mass densities greater than that of atomic nuclei and magnetic fields approaching the electron-positron pair production limit making them distant particle physics laboratories. When these high density objects are in close orbits with other stars, especially other neutron stars, they become fantastic laboratories for testing theories of gravity, such as General Relativity. The high velocities and spins imparted to neutron stars provide fossil clues about their origin. Distances and velocities of these objects figure crucially in many neutron star research areas, including all of the above.

Most known neutron stars are radio-emitting pulsars owing to their regular pulses that provide unique signatures for detection. Normal isolated pulsars have spin periods usually between 20 ms and 2 s. Recycled pulsars, those that have undergone ‘spin-up’ by accretion of matter from a companion star, have spin periods as short as 1.6 ms. This paper will concentrate mainly on normal pulsars.

2. Pulsar timing

Accurately measuring the arrival times of pulses can yield a wealth of information about a pulsar. A measure of the period P and its period derivative \dot{P} provides estimates for the age, $\tau_{\text{char}} = P/2\dot{P}$ and magnetic field, $B \sim 3.2 \times 10^{19} \sqrt{P\dot{P}}$ (in Gaussian units). The changing pathlength caused by Earth orbiting the sun imparts a one year period modulation of magnitude $\sim 500 \text{ s} \cos \beta$ to the timing measurements. The magnitude of the modulation reveals the ecliptic latitude β of the pulsar and the phase provides its ecliptic longitude. A pulsar’s proper motion may be derived by observing the change in these parameters over a very long period (possibly decades). Timing noise limits the precision of timing-derived proper motions to a few milliarcseconds (mas) per year for normal pulsars (cf. Hobbs et al. 2004). The much older recycled pulsars have very little

timing noise and hence can provide astrometry that is up to 100 times better, which in some cases can even measure the curvature of the pulse wavefront providing timing parallaxes.

Pulse arrival times are different at different observing frequencies. This is due to propagation through ionized interstellar medium (ISM) which imparts a delay of $4.12 \times 10^3 \text{ s} \frac{\text{DM}}{\nu^2}$ at a frequency ν in MHz for a dispersion measure of DM measured in parsecs cm^{-3} . The DM is the integrated column density of electrons along the line of sight. A simple model of the electron distribution within the Galaxy (Taylor & Cordes 1993; Cordes & Lazio 2002) provides a method to estimate the distance to a pulsar based on its readily measured DM. Pulsars with known distances are crucial in determining the details of the electron density models, making independent distance measurements important. Based on parallax measurements of nearby pulsars, this model is thought to produce distances accurate to about 40% (Brisken et al. 2003b). Distances to pulsars that are far from the galactic plane ($|z| > 150 \text{ pc}$) are even less accurate.

3. VLBI

The desire for angular resolution at radio wavelengths that is comparable with that of optical instruments has led to the development of large radio interferometers such as the Westerbork Radio Synthesis Telescope, the Australia Telescope Compact Array, and the Very Large Array with baselines up to 30 km, providing arcsecond resolution at frequencies as low as 1.5 GHz. Nothing fundamentally prevents even larger arrays from producing measurements at even higher resolution. The practical problems of transporting data and synchronizing clocks at distant stations have led to what is now known as Very Long Baseline Interferometry. VLBI has become a mature science with NRAO† Very Long Baseline Array (VLBA) operating as a dedicated VLBI array and other consortia of radio telescopes scheduling several VLBI sessions per year. Below is a very brief description of some of the standard methods used to calibrate and image radio interferometry data. These basic techniques are described in much more detail in *Synthesis Imaging in Radio Astronomy II* (1999).

3.1. Visibilities and imaging

The fundamental measurement made by a radio interferometer is the fringe visibility, a complex number produced by combining two antennas' voltage sampled data streams, E_i and E_j at a correlator and integrating the correlation function over a time T ,

$$V_{ij} = \langle E_i(t) E_j^*(t) \rangle_T. \quad (3.1)$$

An N element array produces $N(N-1)/2$ independent visibility measurements for each integration time. Most modern correlators are spectral line correlators, concurrently producing visibilities for each of several frequency channels. The projected baseline vector, (u, v) , is recorded with each visibility measurement for use in imaging and astrometry.

The visibility measured by a pair of antennas is the measurement of a single spatial frequency component of the brightness distribution,

$$V_\nu(u, v) = \int \int \frac{I_\nu(l, m)}{\sqrt{1-l^2-m^2}} e^{-2\pi i \nu (ul+vm)/c} dl dm, \quad (3.2)$$

where (l, m) are the direction cosines parameterizing the sky distribution, and c is the

† The National Radio Astronomy Observatory is a facility of the National Science Foundation operated under cooperative agreement by Associated Universities Inc.

speed of light. A collection of visibility measurements can be inverse Fourier transformed to reveal a ‘dirty’ image of the sky in the direction of interest. The point spread function is readily determined by Fourier Transforming the (u, v) plane sampling. The ‘Clean’ algorithm can then be used to deconvolve the dirty image, restoring the brightness distribution, $I_\nu(l, m)$. For this inversion to be faithful, an appropriate sampling of the visibility function, $V_\nu(u, v)$ must be made. Earth’s rotation causes each pair of antennas to trace elliptical paths in the (u, v) plane.

3.2. Phase-referencing

VLBI data is notoriously difficult to calibrate properly, though better hardware, improved algorithms, and increased bandwidth has over the years have simplified its use greatly, especially for imaging experiments. Astrometry remains quite tricky, especially at frequencies below 2 GHz where the ionosphere can cause rapid phase fluctuations and at frequencies greater than 15 GHz where the troposphere causes similar grief.

The simplest form of calibration, phase-referencing, involves nodding the antennas between a bright point-like calibrator source of accurately known position and the potentially much weaker target source. The nodding time depends on frequency but ranges usually between 30 s and 5 min. The visibility corresponding to a single point source at location (l, m) relative to the center of the field of view is

$$V_\nu^{\text{point}}(u, v) = \frac{S_\nu}{\sqrt{1 - l^2 - m^2}} e^{-2\pi i \nu (ul + vm)/c}, \quad (3.3)$$

Where S_ν is the source flux density. Calibration involves determining in a least-squares sense the *station-based* complex gain factors, g_i that minimize

$$\chi^2 = \sum_{i,j} |g_i g_j^* V_{ij}^{\text{observed}} - V_{ij}^{\text{model}}|^2 \quad (3.4)$$

by observing a calibrator source with known V_{ij} . Calibration proceeds by interpolating the complex gains derived from the calibrator observations and applying them to the target observations. The amplitudes are almost always more stable than the phases in VLBI observations, and it is the phases that contain the astrometric information, so the remainder of this section will focus on phase calibration.

3.3. In-beam calibration

Phase-referencing leaves uncorrected spatial gradients in the phase front caused by the non-uniform ionosphere and troposphere. The calibration is improved by observing a calibrator source as near the target as possible. At the lower frequencies, where the primary beam of the individual telescopes is large enough, one can often find with the aid of Very Large Array imaging compact sources within the same primary beam as the target. These sources can be much weaker (10 mJy rather than about 80 mJy at 1.5 GHz) since the bulk of the phase variation can be removed by nodding to a brighter, more distant calibrator. This technique was first used on a pulsar in the parallax measurement of B0919+06 by Chatterjee et al. (2001).

3.4. Ionosphere calibration

At frequencies below about 5 GHz, the phase fluctuations are dominated by the ionosphere. The phase of a visibility of a point source at location (l, m) on a baseline (u, v) at frequency ν is

$$\phi = \frac{\nu}{c} (u l + v m) + \epsilon(\alpha, \delta, t, \nu) + \text{noise}. \quad (3.5)$$

The error term, ϵ has contributions from the troposphere, the ionosphere, and the instrument,

$$\epsilon(\alpha, \delta, t, \nu) = \underbrace{A(\alpha, \delta, t) \cdot \nu}_{\text{Troposphere}} + \underbrace{B(\alpha, \delta, t) \cdot \nu^{-1}}_{\text{Ionosphere}} + \underbrace{C(\alpha, \delta, t, \nu)}_{\text{Instrument}}. \quad (3.6)$$

The contribution from the instrument is very stable for modern antenna arrays and can usually be considered constant. Since the phase error due to the ionosphere has a different frequency dependence ($\propto \nu^{-1}$) than that of the troposphere or any other pure delay ($\propto \nu$), it can be measured and removed given a strong enough target source whose observations span a large enough frequency range. Note that the geometric term that is being determined has a frequency dependence identical to that of a pure delay making a similar calibration for the troposphere not possible. A similar technique can be used by simultaneously observing at 2.3 and 8.4 GHz. Pulsars are too weak to be observed at these frequencies, but there is enough bandwidth to span in the 1.2 to 1.7 GHz band. This technique was developed for measuring the parallax to pulsar B0950+08 (Brisken et al. 2000), see Fig. 1 and has been extended to determine parallaxes for 8 other pulsars (Brisken et al. 2002).

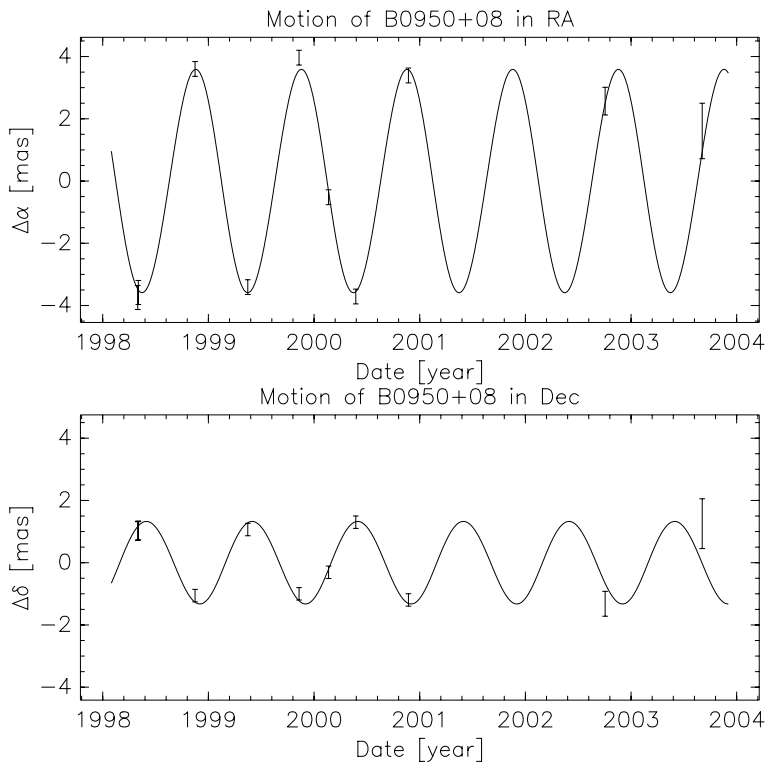


Figure 1. The parallax fit of Pulsar B0950+08 using ionosphere calibration (Brisken et al. 2000). The proper motion and parallax values fit for this pulsar are $\mu_\alpha = -2.07 \pm 0.07 \text{ mas yr}^{-1}$, $\mu_\delta = 29.37 \pm 0.05 \text{ mas yr}^{-1}$, and $\pi = 3.81 \pm 0.07 \text{ mas}$ respectively. Note that the fit proper motion has been subtracted to show more clearly the parallax.

4. The VLBA

The VLBA consists of ten identical 25-m radio telescopes operating between 327 MHz and 90 GHz. The maximum baseline is 8600 km, yielding 5×11 milliarcsecond (mas) resolution at 1.5 GHz for sources at moderate ($\sim 20^\circ$) declination. It nominally observes over a 32 MHz bandwidth, but can observe at twice or four times that bandwidth at a correspondingly reduced duty cycle. Because of its year-round availability, simple scheduling, flexible tuning capabilities and reliable operation it has been the instrument of choice for pulsar VLBI observations.

4.1. VLBA pulsar observations

Pulsars have very steep spectra, $S_\nu \propto \nu^{-\alpha}$ for $1 < \alpha < 2.5$ usually. Thus pulsar observations are usually made at ~ 1.5 GHz or sometimes 5 GHz as a compromise between source brightness and instrument resolution. Scattering, especially near the Galactic center, can be a problem at frequencies below 5 GHz. As observing bandwidths increase, the observing frequency will likely increase as calibration is easiest around 8 GHz. The VLBA correlator in Socorro, NM has a pulsar gate which allows a factor of 3 to 5 increase in signal-to-noise ratio by blanking the signal inputs to the correlator during the off-pulse portions of each pulsar rotation.

5. Applications of pulsar astrometry

The following sections describe some applications of pulsar astrometry and some recent results.

5.1. Pulsar velocity distribution

Pulsars have typical velocities of 100 to 300 km s^{-1} , far faster than the class of stars thought to be their progenitors. It is fairly clear based on this simple observation and on positional properties of pulsar-supernova remnant associations that supernovae impart significant momentum to the pulsars they form. Determining the distribution of pulsar birth velocities would improve our understanding of the core collapse process.

Sample biases greatly challenge any effort to measure the distribution of velocities. Many proper motion studies are biased toward the brighter, easier to study pulsars, biasing toward the slower moving pulsars that loiter in the solar neighborhood. The more distant pulsars tend to be traveling more along the line of sight than in the plane of the sky. Since only the transverse velocity is amenable to observation, this tends to lower the observed velocity. Also pulsars with large z velocities tend to leave the sample volume, whereas pulsars with velocities parallel to the plane of the Galaxy tend to enter and leave the sample volume at almost the same rate. Dispersion measure based distances are inaccurate for pulsars with $|z| > 200$ pc since they are above the bulk of the Galactic electron content.

Brisken et al. (2003b) measured proper motions of twenty eight pulsars using the VLA. Wide-field images made at 1.4 GHz typically contain about 15 compact ($< 1''$) background objects that were used to define a coordinate grid on the sky near the pulsar. The pulsar's motion against this grid of points can then be measured to a precision of roughly 1 to 10 mas yr^{-1} , depending on the brightness of the pulsar and somewhat on its location in the sky. These results were combined with six additional pulsars with high quality VLBI proper motions and parallaxes in a velocity distribution analysis. In order to minimize the bias related to pulsars with large z velocities, only the velocity component parallel to the plane of the Galaxy was used. This also avoids the need to disentangle acceleration due to the gravitational potential of the Galaxy from the velocity.

Several model forms were fit to the observed proper motion and distance estimates. The best fit among those tested was a velocity distribution with two normally distributed components. The values obtained compared reasonably with an independent method that used forward evolution of a sample of pulsars to determine the model (see Fig. 2).

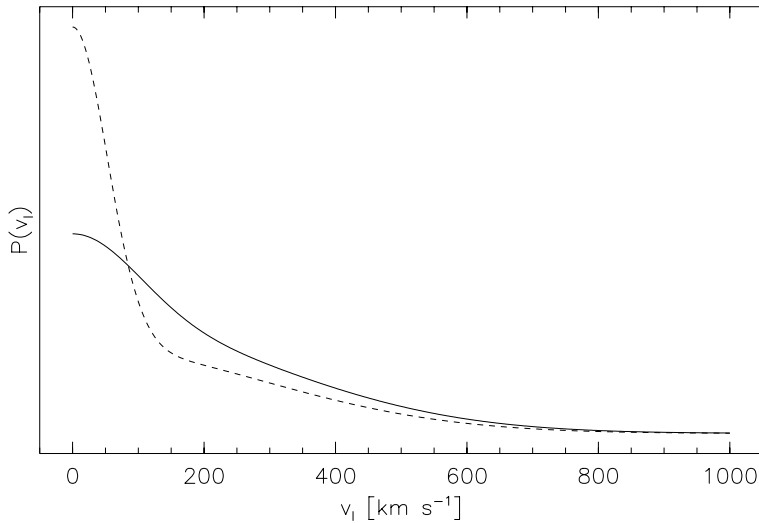


Figure 2. The best fit velocity distribution from Brisken et al. (2003b) is shown by the solid curve. In this distribution, 20% of pulsars are contained in a normal distribution with a width of 99 km s^{-1} and the remainder in a normal distribution of width 294 km s^{-1} . This is compared to the fit of Arzoumanian et al. (2002) shown dashed. They found 40% in a 52 km s^{-1} distribution and 60% in a 289 km s^{-1} distribution.

5.2. Galactic electron distribution

The ionized interstellar medium retards the arrival of radio waves by an amount Δt given by

$$\Delta t = \frac{e^2}{2\pi m_e c \nu^2} \int_0^d n_e dl, \quad (5.1)$$

where m_e and e are the mass and charge of an electron, ν is the frequency of observation, and n_e is the local electron density. The total integrated column density of electrons toward a pulsar is called the dispersion measure (DM) and is directly observable with multi-frequency timing observations. Thus given a model for the electron distribution within the Galaxy, $n_e(d, l, b)$ and the DM, one can determine the pulsar's distance. Using limited pulsar distance data, the distribution of pulsar dispersion measures and other physical constraints, Taylor & Cordes (1993) published a model of the Galactic electron distribution that included spiral arms.

Recent VLBI parallaxes, as well as parallaxes derived from the timing of stable millisecond pulsars, a large number of new pulsar discoveries, more and improved scattering measurements as well as a handful of other constraints have yielded a newer model called NE2001 (Cordes and Lazio 2001). Ongoing VLBI parallax measurements will likely again double the number of direct parallax distances and improve the model details out to greater distances. See Fig. 3.

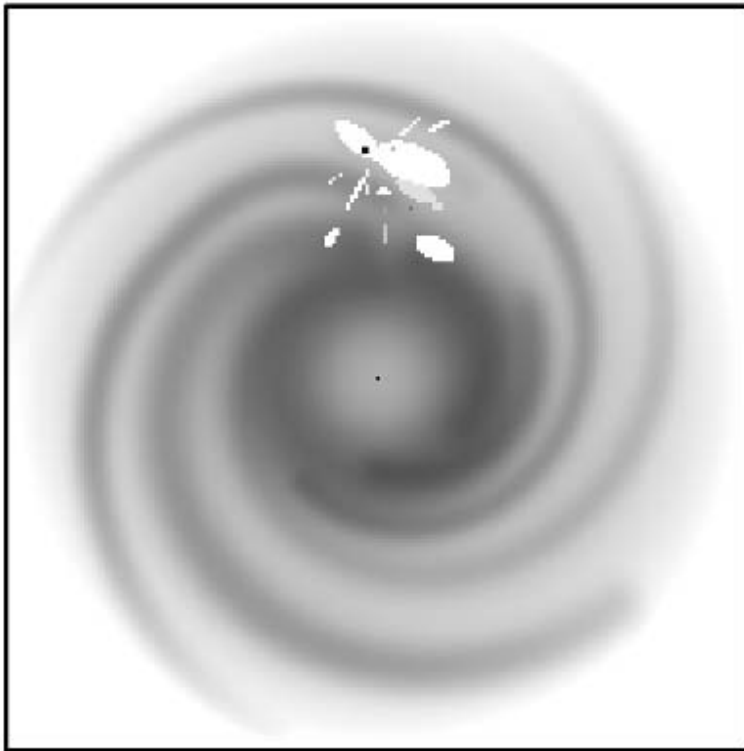


Figure 3. The Galactic electron density plotted over an area of $30 \times 30 \text{ kpc}^2$. The greyscale levels are logarithmic. Around the solar neighborhood, small structures have been modeled such as the Gum Nebula and Vela SNR. Also some local low density regions have been included in the model. Figure is from Cordes & Lazio (2002).

5.3. Pulsar / supernova remnant association

Pulsars and supernova remnants provide complementary information about supernova explosions when two such objects can be connected. The SNR provides information about the ISM local to the supernova and can in some cases be used to obtain distance and age information. The pulsar's proper motion can be used to determine the center-point of the explosion. Pulsar astrometry has recently firmly established three pulsar/SNR associations. Since the discovery of Pulsar B1951+32 its association to SNR CTB80 has been assumed based on the apparent interaction of the two objects (see Fig. 4). A recent proper motion by Migliazzo et al. (2002) has confirmed the predicted direction of motion of the pulsar. Using long term timing data for pulsar J0538+2817, its association with SNR S147 has been strengthened (Kramer et al. 2004). This association has led to a measurement of this pulsar's initial spin period of 139 ms based on its age and proper motion.

The distance to pulsar B0656+14 was sought because of the possibility of a radius measurement for this object (see section 5.5). This pulsar lies near the center of the Monogem ring, a large X-ray bright ring that was confirmed to be a SNR by Plucinsky et al. (1996). Models place the ring at a distance of about 300 pc. The association of these two objects was not initially considered due to the discrepant distances when using the pulsar's DM as a proxy for its distance. A five-epoch VLBA observation using a bright in-beam reference source yielded a distance of 288_{-27}^{+33} pc (Briskin et al. 2003a). Thorsett

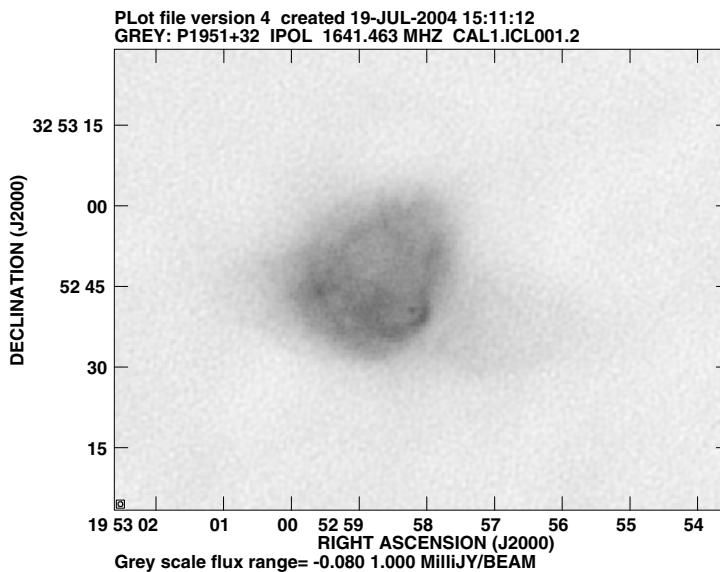


Figure 4. The central region of SNR CTB80. Pulsar B1951+32 (point source near lower right of the central nebula) was found to be moving toward the arc-like structure right of the pulsar. The nature of this arc is still uncertain. Image courtesy of Ben Zeiger, made from archival VLA data.

et al. (2003) revived the association hypothesis and with this provided an age for the Monogem ring.

5.4. Core collapse

Supernova core collapse leaves its signature in the large velocities and the spins of the pulsars they produce. The misalignment angle of a pulsar's spin and velocity vectors probes the process by which a neutron star is kicked. Most models that produce the significant velocities that are observed require the collapse to be asymmetric. Spruit & Phinney (1998) postulated that this asymmetry would cause correlation between spin and velocity that could be observed. With the advent of high-resolution X-ray imaging from space, the spin axes of young pulsars can be probed by examining the symmetry of the X-ray wind nebula surrounding some pulsars. This involves fitting observed X-ray data to models consisting of one or two equatorial disks and/or polar jets (Romani & Ng 2003; Ng & Romani 2004; see Fig. 5). Combined with high precision astrometry of the pulsar, this idea is now being tested. The spin-velocity misalignment angle is plotted against measured initial spin period for 5 pulsars in Fig. 6. These suggest that the timescale over which rotational averaging aligns the two vectors is about 2 to 3 s.

5.5. Neutron star properties

The determination of some neutron star properties, such as luminosity, depend directly on the distance to the pulsar. Pulsar B0656+14 is an X-ray bright source consisting of a two-component blackbody and a power-law spectrum. The two blackbody components are interpreted as those from the neutron star surface and the hotter polar caps; the power-law is likely magnetospheric in origin. Recent fits for the surface temperature by Marshall & Shultz (2002) suggest a surface temperature of $T_{\infty} = 8.0 \pm 0.3 \times 10^5$ K. A distance measurement would allow a direct radius measurement given the well determined blackbody measurements. The distance of 288 pc measured with the VLBA implies a

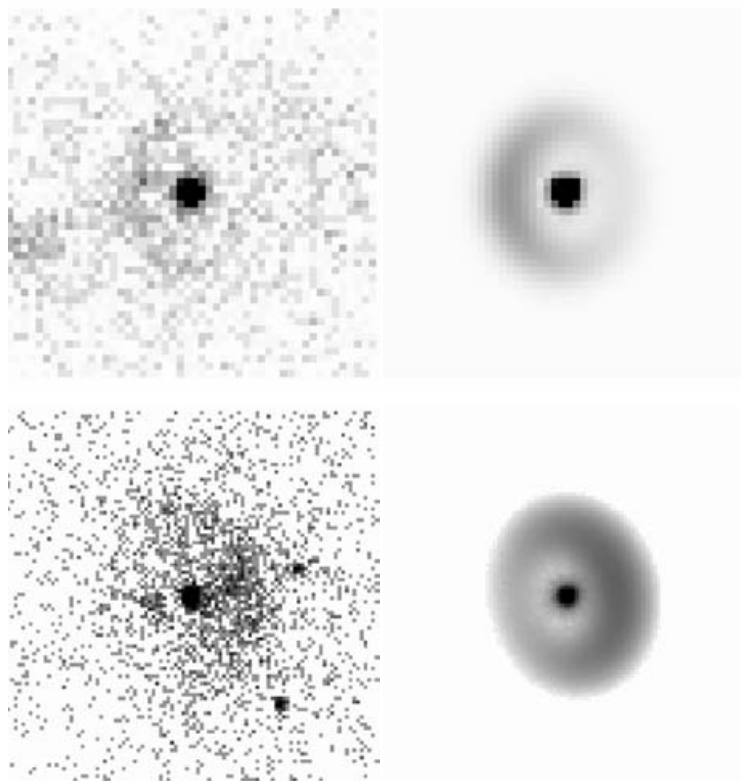


Figure 5. Top: a cleaned Chandra X-ray Observatory image of Pulsar J1930+1852 and its best fit one-disk model. Bottom: The same for Pulsar J2229+6114. Images courtesy of Roger Romani.

blackbody radius in the range 6.9 to 8.5 km, depending on the details of the modeling (Briskin et al. 2003a). Since this radius is not supported by any reasonable neutron star equation of state, this measurement was turned around and used as a probe of the neutron star atmosphere, which distorts the blackbody spectrum. A fit by Anderson et al. (1993) using a magnetized hydrogen atmosphere model of Shibunov et al. (1993), places the radius at $R_\infty = 13$ km given the new distance measurement, which is consistent with the canonical neutron star radius. Given uncertainties in the modeling, any radius between about 13 and 20 km is allowed by the observations.

Acknowledgements

I'd like to thank Don Kurtz and Gordan Bromage for organizing such an interesting conference that addressed a wide range of interests and for providing such a unique opportunity to view the Transit of Venus in historical context.

References

- Anderson, S. B., Córdova, F. A., Pavlov, G. G., Robinson, C. R. & Thompson, R. J. Jr. 1993, *ApJ*, 414, 867
 Arzoumanian, Z., Chernoff, D. F., & Cordes, J. M. 2002, *ApJ*, 568, 289
 Briskin, W. F., Benson, J. M., Beasley, A. J., Fomalont, E. B., Goss, W. M. & Thorsett, S. E. 2000, *ApJ*, 541, 959

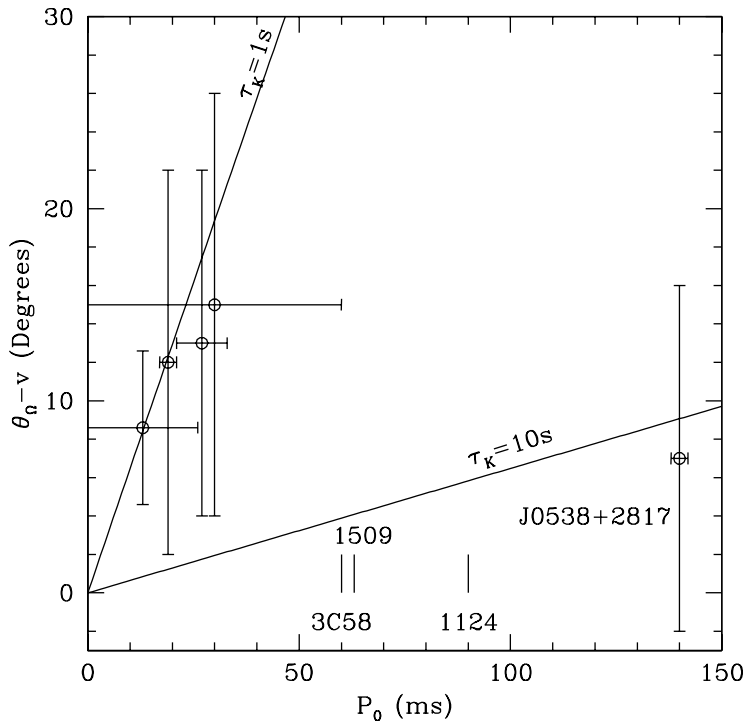


Figure 6. Spin-velocity angle misalignment plotted against pulsar initial spin period for 5 pulsars. These data suggest a 2- to 3-s kick duration.

- Brisken, W. F., Benson, J. M., Goss, W. M., & Thorsett, S. E. 2002, *ApJ*, 571, 906
- Brisken, W. F., Thorsett, S. E., Golden, A., & Goss, W. M. 2003a, *ApJ*, 593L, 89
- Brisken, W. F., Fruchter, A. S., Goss, W. M., Herrnstein, R. M., & Thorsett, S. E. 2003b, *AJ*, 126, 3090
- Chatterjee, S., Cordes, J. M., Lazio, T. J. W., Goss, W. M., Fomalont, E. B. & Benson, J. M. 2001, *ApJ*, 550, 287
- Cordes, J.M. & Lazio, T. J. W. 2002, astro-ph/0207156
- Hobbs, G., Lyne, A. & Kramer, M. 2004, *IAU Symposium* 218, 431
- Kramer, M., Lyne A. G., Hobbs, G., Löhmer, O., Carr, P., Jordan, C., & Wolszczan, A. 2004, *ApJ*, 593L, 31
- Marshall, H. L. & Shultz, N. S., 2002, *ApJ*, 574, 377
- Migliazzo, J. M., Gaensler, B. M., Backer, D. C., Stappers, B. W., van der Swaluw, E. & Strom, R. G. 2002, *ApJL*, 567, L141
- Ng, C. Y. & Romani, R. W. 2004, *ApJ*, 601, 479
- Plucinsky, P. P., Snowden, S. L., Aschenback, B., Egger, R., Edgar, R. J., & McCammon, D. 1996, *ApJ*, 463, 224
- Romani, R. W. & Ng, C. Y. 2003, *ApJ*, 585L, 41
- Shibunov, Y. A., Zavlin, V. E., Pavlov, G. G., Ventura, J. & Potehkin, A. 1993, in *Isolated Pulsars*, eds. Van Riper, K. A., Epstein, R. I., & Ho, C., Cambridge University Press, 174
- Spruit, H. C. & Phinney, E. S. 1998, *Nature*, 393, 139
- Synthesis Imaging in Radio Astronomy II, eds. Taylor, G. B., Carilli, C. L. & Perley, R. A. 1999, ASP conf. series 180
- Taylor, J. H. & Cordes, J. M. 1993, *ApJ*, 411, 674
- Thorsett, S. E., Benjamin, R. A., Brisken, W. F., Golden, A., & Goss, W. M. 2003, *ApJ*, 592L, 71

Discussion

MIKHAIL MAROV: You're completely right saying that the ionospheric, and partially tropospheric, effects crucially influence the accuracy of data collected, and you also mention that GPS suffers very much from that. It is a most important component influencing the data accuracy. So GPS people are now eliminating, or at least decreasing, the effect using a multiple – say double or triple – frequency approach. Will the same idea improve the data accuracy of VLBI?

WALTER BRISKEN: That's right. We are doing this in two stages: The first uses the published maps from GPS observations to calibrate out the bulk of the delay, while leaving us just differential uncorrected data. The other is that geodesists and other astrometrists have been using dual frequency observations for many years. Usually at S-band at 2.4 GHz and X-band at 8 GHz; this has worked very well. A technique I developed from my thesis is to use multiple frequencies within just the L-band at 1.4 GHz and 1.7 GHz; the signature of the ionosphere is so strong at these lower frequencies that just within that 300 MHz we can already measure and remove the effect of the ionosphere.

MIHAIL MORAV: Is it then possible to avoid drifting anomalies in the ionosphere, or some kind of irregularities stirred up by solar activity, especially sudden disturbances?

WALTER BRISKEN: Yes, we have actually observed these MSTIDs – medium scale travelling ionospheric disturbances (as they are called). If you map the magnitude of the differential ionosphere on 30-second timescales, you see many degrees of phase change. So we do see those, and we are in some cases able to correct for them.

CORYN BAILER-JONES: I'd heard that somebody had been using VLBI of radio stars to look for exo-planets. Do you know anything about this?

WALTER BRISKEN: I have not heard about that observation. I assume it's using the wobble technique. I suppose if you are able to get it at 8 GHz where the ionosphere is less problematic and your resolution is five times higher, then you should easily be able to get down to 50 micro-arc seconds resolution. Recently someone demonstrated 10 micro-arc second astrometry in the measurement of the speed of gravity. It's something you may have heard about where Jupiter passed very near a quasar. They wanted to look for the apparent motion of the quasar as a result of Jupiter's gravity influence. So 10 micro-arc seconds is currently the state of the art and I assume that people have started to use this to look for exo-planets. But it's not a very easy technique – there's a lot of work involved – so it's probably not done on more than 10 objects or so at a time.

DON KURTZ: Walter, if I can go back to Monday when Myles and Lena told us we know the astronomical unit to a precision of metres: Let's pretend that we didn't have their technique. We know that ten years ago planets were artificially discovered around a pulsar because the barycentre correction was wrong. How precisely could you determine the AU with your parallaxes?

WALTER BRISKEN: That's a good question. Unfortunately, none of the pulsars that have timing distances also have VLBI distances, but I guess those are probing the same AU anyway. I'm not actually sure what you would do.

DON KURTZ: If the astronomical unit were wrong – if you had the barycentre in the wrong place – you would see an annual motion in your positions for the pulsar. So, at

what level would you detect that, was the question. For the public that might be an interesting number to know. I was very intrigued when you said that you can pick up the angular momentum change in the Earth when you release water from a dam. At what level are you timing the Earth's period with the VLBA?

WALTER BRISKEN: The Earth orientation service does make daily, maybe hourly measurements of the orientation of the Earth and it shows up in this data. Maybe Myles Standish knows more?

DON KURTZ: Myles, do you know the Earth's period to micro-second precision, nano-second precision?

MYLES STANDISH: [response unrecorded]

DON KURTZ: Then how can you detect the change in the Earth's rotation rate with just the release of water from a dam?

MYLES STANDISH: I don't know. I didn't say that!

[general laughter]

DON KURTZ: I think that it's a change at the level about a millisecond for El Niño – but that's from massive flows in the Pacific – so it's an amazing claim.

WALTER BRISKEN: I think it's micro-seconds accuracy. We can get the axis of the Earth in the reference frame of the ICRF to the order of 100 or maybe 10 micro-arcseconds, and if it's an effect that integrates with time such as a rotation rate – then observations over a period of time may show this effect.



Walter Brisken observing the transit